Automated image analysis techniques for cardiovascular magnetic resonance imaging

Geest, R.J. van der

CHAPTER

5

Assessment of regional left ventricular wall parameters from short axis MR imaging using a 3D extension to the improved Centerline method

This chapter was adapted from:

Assessment of regional left ventricular wall parameters from short axis MR imaging using a 3D extension to the improved Centerline method
Vincent G.M Buller, Rob J. van der Geest, Martin D. Kool,
Ernst E. van der Wall, Albert de Roos, Johan H.C. Reiber
Investigative Radiology 1997, Volume 32, Issue 9, Pages 529-539.

ABSTRACT

Rationale and objectives: Short-axis magnetic resonance images of the cardiac left ventricle, acquired in multiple slices and phases, may be used for the quantitative assessment of regional wall parameters. Conventional two-dimensional (2D) methods for wall thickness measurement rely on information within one imaging plane which may result in overestimation of the true thickness depending on the local direction of myocardial wall with respect to the imaging plane.

Methods: In order to perform wall thickness measurements truly perpendicular to the myocardial wall, a three-dimensional (3D) wall thickness calculation algorithm has been developed based on the 2D improved centerline method. An evaluation was performed on left ventricular-shaped software phantoms, and on the MRI data obtained from 20 healthy individuals.

Results: The 3D method applied to software phantoms with an angulation within 20° of the true short-axis orientation demonstrated only a 1.6% overestimation of wall thickness at the mid to low slices, and a 10.6% error at the apex (2D measurements: 8.1% and 28.6%, respectively). Three-dimensionally calculated wall thickness in the healthy individuals was systematically and significantly smaller than corresponding 2D wall thickness (by 11.2%, 8.7% and 2.6% at the apical, low and mid slices, respectively).

Conclusions: Cardiac wall thickness measurements from short-axis MR studies can be obtained with a higher accuracy by the newly developed 3D approach than with the conventional 2D approach.

5.1 Introduction

Cardiac magnetic resonance (MR) has been generally accepted as an accurate and reproducible modality for the quantitative evaluation of left ventricular (LV) function. Multi-slice, multi-phase (MSMP) MR acquisitions have been found suitable for the accurate assessment of left ventricular volumes[1-3] and mass[4,5], as well as for the assessment of local functional parameters such as wall thickness and wall thickening or thinning[6].

Magnetic resonance imaging acquisitions, in particular in the short-axis orientation, have proven their usefulness for the determination of regional wall parameters[7-10]. Local wall thickness can be derived from these acquisitions by manual or automatic outlining of the endocardial and epicardial boundaries in each short-axis image[9,11,12]. Because true wall thickness is only acquired when measurements are performed perpendicular to the myocardium, achieving this within-image perpendicularity is the goal of advanced two-dimensional (2D) algorithms such as the improved centerline method (Figure 5-1)[13,14].

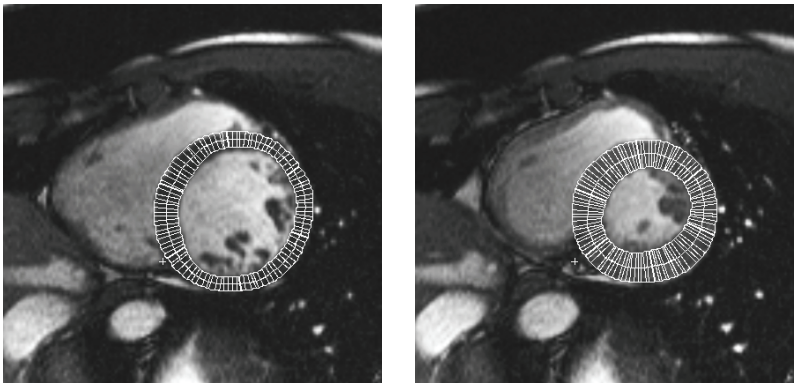

Figure 5-1. A typical short-axis image of a normal individual in the end-diastolic (left) and end-systolic (right) phases of the cardiac cycle with manually drawn contours and centerline chords for planar wall thickness measurement.+ indicates the posterior junction of the right ventricle with the left ventricular wall, where the clockwise numbering of the 100 centerline chords was started

Because such methods are confined to measurements within individual 2D images, the implicit assumption is made that the myocardial wall itself is always perpendicular to the acquisition plane. However, because of the ellipsoidal cardiac geometry this assumption is rarely true, even when true short-axis images are obtained. In particular near the apex, the myocardium exhibits a through-plane curvature which causes the

myocardium and imaging plane to intersect at an oblique angle. Planar, 2D wall thickness methods will therefore inevitably overestimate true wall thickness in a systematic manner (Figure 5-2A). In addition, a randomly distributed error may be introduced in 2D wall thickness measurements in every individual slice if different myocardial regions are inclined differently to the imaging plane. This effect may either occur due to cardiac geometry or be caused by an inaccurate determination of the short-axis orientation (Figure 5-2B).

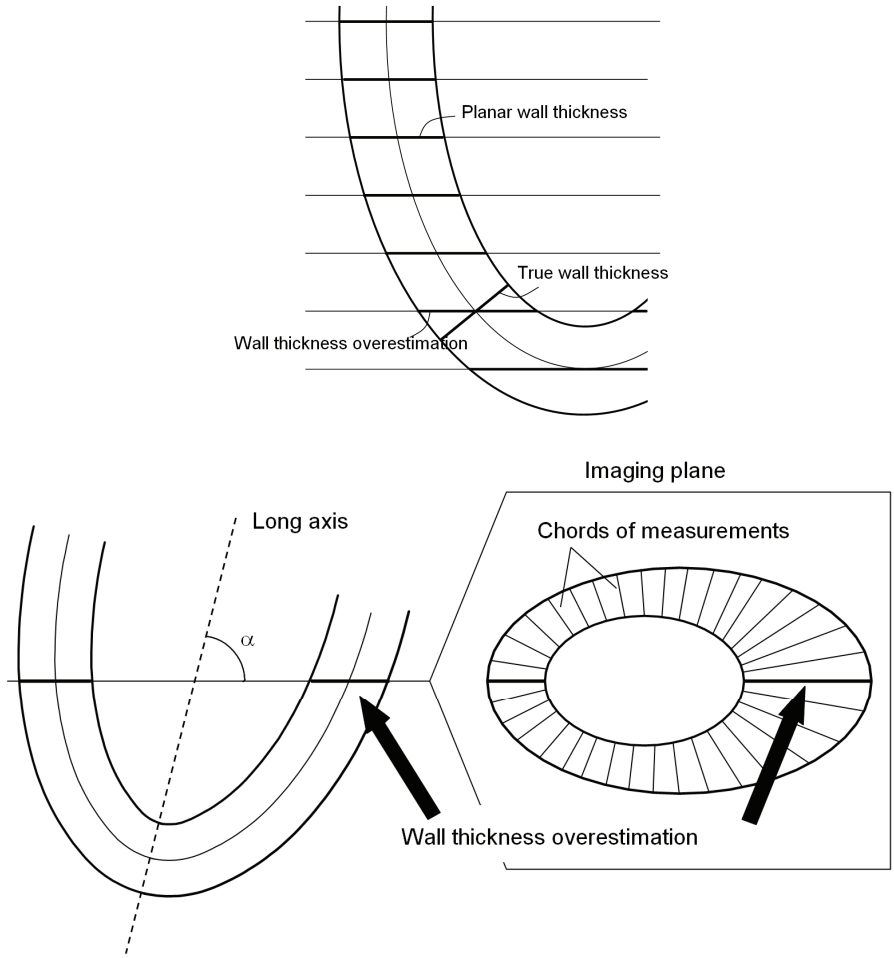

Figure 5-2. (A) Planar wall thickness measurements will overestimate true wall thickness in the lower slices of the left ventricle. The degree of overestimation depends on the angle [alpha], which should be 90° in the ideal situation. (B) Planar wall thickness accuracy will vary along the circumference of the myocardial wall if different segments of the wall have a different inclination with the imaging plane-for example, because of an imprecisely determined short-axis orientation.

However, the myocardial boundaries of a multi-slice, multi-phase MRI acquisition contain three-dimensional (3D) shape information which may be used to prevent both these systematic and random overestimations (Figure 5-3). Therefore, a new 3D wall thickness calculation algorithm has been developed to measure wall thickness always perpendicular to the myocardium, and thus to effectively estimate true wall thickness. In comparison to the existing planar methods, this method was expected to demonstrate a decreased wall thickness in the apical slices, and an increased wall thickness homogeneity within individual images.

In normal patient studies, the new 3D algorithm was expected to decrease wall thickness inter-subject variation because its results would be independent of the cardiac geometry and the orientation of the MR acquisitions. Consequently, 3D calculated wall thickness would result in smaller normal value ranges. The comparison of wall thickness in patients to these smaller normal value ranges may lead to higher sensitivities and specificities in the assessment of the extent and severity of dysfunctional myocardium in patients.

The purpose of this study was an evaluation of the newly developed 3D wall thickness method based on software phantoms as well as on multi-slice, multi-phase short-axis MR acquisitions obtained from 20 healthy individuals.

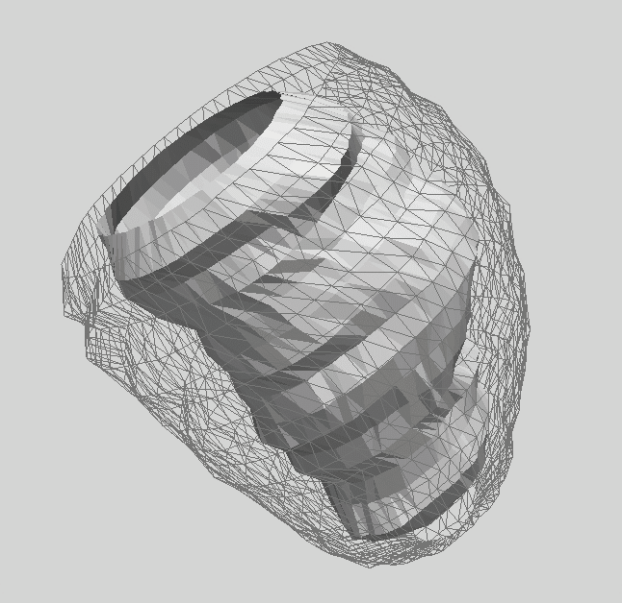

Figure 5-3. A short-axis, multi-slice magnetic resonance imaging acquisition comprises a detailed three-dimensional description of the cardiac left ventricle.

5.2 MATERIALS

5.2.1 The software phantoms

In order to compare the accuracy and precision of the 3D wall thickness method with the conventional 2D method and the true wall thickness values, a software phantom with an overall true wall thickness of 10 mm was constructed. The phantom was given an approximate end-diastolic left ventricular shape and size to ensure a natural occurrence of systematic and random errors in the two-dimensional measurements. To this purpose, the lower portion of the phantom was modeled as an ellipsoid of 70 mm epicardial height, extended at the base by a cylinder with an epicardial diameter of 70 mm (Figure 5-4). The phantom was given a vertical, true short-axis orientation. Twelve similar phantoms were each created at a different, unique tilt angle from the short-axis orientation (from 5° to 60°, in 5° increments).

All phantom study imaging parameters were chosen similar to the in-vivo normal acquisitions used in this study. The image resolution was 256×256 pixels at a field of view of 400×400 mm², resulting in an average wall thickness of 6.4 pixels. Slice thickness was 10 mm with no inter-slice distance. Slice number 1, the lowest slice, was acquired at the epicardial point of the apex. The slices at levels 2, 3, 5 and 7, representing the apical, low, mid and basal slices of a normal left ventricle, were selected for analysis.

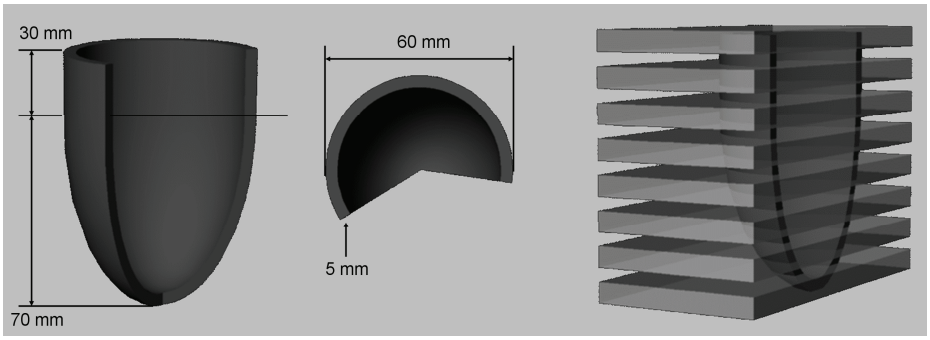

Figure 5-4. The 13 software phantoms were created for the in vitro study. The dimensions of all software phantoms were identical, but only the angle of acquisition was different for each.

5.2.2 In-vivo study data

Twenty normal individuals were selected based on the criteria defined in the Framingham trial[7]. Each included individual had a normal ECG and no

clinical signs or history of cardiac disorder. The mean age for the group was 37.4 years (range 21-78). The gradient-echo MRI studies were acquired on 0.5T (10 cases) and 1.5T (10 cases) MR scanners using the body coil (Philips Medical Systems, Best, The Netherlands). The short-axis orientation was determined by visual inspection of end-diastolic (ED) and end-systolic (ES) phases in a four chamber scout view, such that the short-axis imaging slices were selected perpendicular to the left ventricular long axis. The images were acquired at a field of view of 400x400 mm² and an image resolution of 256×256 pixels. Ten slices of thickness 10 mm (10 cases) or 8 mm (10 cases) were acquired with either a slice gap of 1 mm (15 cases) or 2 mm (5 cases). From these slices basal, mid, low and apical slices were selected independently in both ED and ES phases based on the following criteria: The basal slice was the second slice from the ventricular base to encompass the complete myocardium; the mid slice was the lowest slice in which papillary muscles were still clearly distinguishable from the myocardium, and the low and apical slices were the second and first slice up from the apex with complete endocardial and epicardial outlines.

5.3 Methods

5.3.1 Software description

5.3.2 The two-dimensional improved centerline method

Two-dimensional wall thickness was calculated with the improved centerline method[13,14]. This planar method allows the assessment of wall thickness at a high resolution, and is independent of generally disregarded geometrical model assumptions such as an approximately circular myocardial shape or a predefined cardiac center point[15]. Instead, the improved centerline method begins by defining a 'centerline' midway between the endo- and epicardial boundaries in each individual image. One hundred measurement chords are then placed at equal distances perpendicular to this centerline. The length of each chord within the myocardium is then a measure of local wall thickness. In a subsequent iterative procedure, crossing chords and other possible anomalies are solved by redistribution and reorientation of the chords in problem areas (Figure 5-1b). The chords were then numbered in clockwise order, starting at the posterior junction of the right ventricle with the LV wall. The independent definition of this starting location in all images at the ED and ES phases compensated for the rotational motion of the left ventricle. Due to the large number of 100 chords per image, a sufficiently high measurement resolution was guaranteed in all images.

5.3.3 The three-dimensional wall thickness calculation

The 3D method extends the planar improved centerline method by incorporating 3D ventricular shape information, and performing wall thickness measurements perpendicular to the ventricular wall.

The 3D method constructs a 3D mid-myocardial surface *S,* describing the shape of the ventricular wall, through all the centerlines calculated by the planar centerline method (Fig 5-5a). By definition, all midpoints of the 2D centerline chords are on this surface *S*. At each of these midpoints a tangent plane *P* is constructed to the surface *S* from an in-plane or horizontal ($\vec{h}$) and a vertical ($\vec{v}$) vector component (Figure 5-5d). The horizontal vector $\vec{h}$ at a particular position is calculated by vector-averaging the centerline chord at hand with its two neighbors and rotating the resulting vector through 90° within the horizontal plane (Figure 5-5b). The vertical vector $\vec{v}$ is derived by averaging the two upward pointing vectors between the midpoint and its closest neighboring points in the two adjacent slices (Figure 5-5c).

Next, the angle α (see Figure 5-2b) between the normal vector of the imaging plane and the normal vector of the constructed plane *P* is calculated. The three-dimensional wall thickness WT_{3D} may then be derived from the 2D wall thickness measurement WT_{2D} using equation 5-1:

$$WT_{3D} = WT_{2D} \times \sin(\alpha) \qquad (5\text{-}1)$$

The basic 3D algorithm described above uses planar measurements from the current slice and its two adjacent slices. A variant algorithm was conceived for the uppermost and lowest slices where only one neighboring imaging slice is present. In these cases the vertical vector $\vec{v}$ is defined to be equal to the vector between the current centerline midpoint and its closest neighboring midpoint in the adjacent slice.

5.3.4 Evaluation methods

Phantom study data

A quantitative evaluation concerning the accuracy and precision of the planar and 3D methods was performed on the software phantom data. To assess the presence and extent of random errors introduced by deviations in short-axis orientation, wall thickness was measured in software phantoms at all given acquisition angles. The 100 chord measurements per slice were averaged, and minimum, maximum and standard deviations

were calculated. In order to also establish the presence and extent of the systematic error due to the curvature of the cardiac wall near the apex, results at 4 different slice levels were determined.

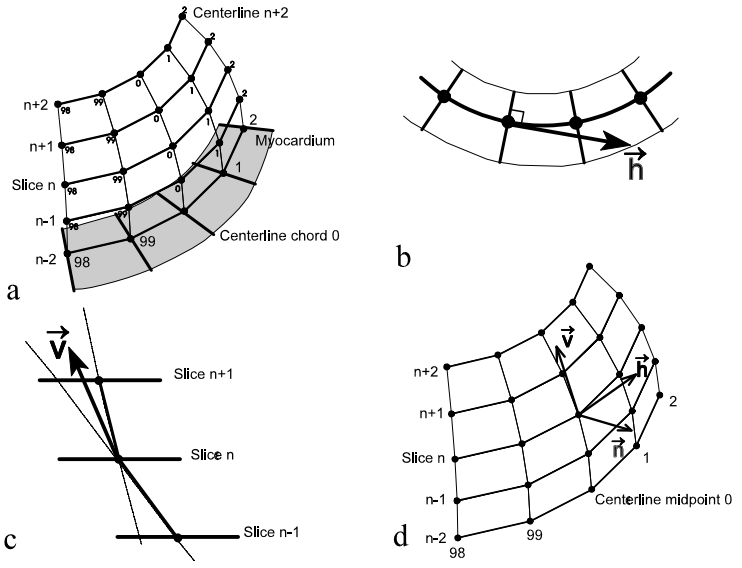

Figure 5-5. (A) A surface can be constructed from a stack of centerlines running midway between the endocardium and epicardium. At each center point on this surface (B) horizontal and (C) vertical direction vectors can be constructed from adjacent centerline chords. (D) These vectors define a plane tangent to the mid-myocardial surface. The angle between the normal vector of this plane and a normal vector of the imaging plane then defines the local inclination between myocardium and imaging plane.

In-vivo study data

In order to determine the effectiveness of the 3D method on clinical data and in the establishment of accurate normal value ranges, a quantitative evaluation was carried out on the in-vivo studies of 20 healthy volunteers.

In each in-vivo study the endocardial and epicardial contours were manually traced by an experienced observer in all images with a completely visible myocardium (distinguishable endocardial and epicardial boundaries, slices only below aortic valve level). These contours were traced to encompass only the myocardial wall, and to exclude papillary muscles and trabeculae. In case the myocardial boundary was imaged with some blurring due to the partial volume effect, the contour location was chosen to be on the center of the visible boundary. All manual analyses were performed under identical lighting conditions and fixed display window and level settings.

In each study ED and ES phases were selected as the first imaged cardiac phase and the phase with the smallest calculated blood pool volume, respectively. Wall thickness was measured with both methods at 100 chord positions in all slices of both phases. The 100 chord measurements per slice were averaged, and minimum, maximum and standard deviations were calculated.

The wall thickness measurements were further grouped into three anatomical regions using the clockwise order of the centerline chords. Starting at the posterior junction of the right ventricle with the left ventricular wall, the first 20% of the chords was considered septal and the next 30% anterior. The remaining 50% was defined a lateral/posterior region. Wall thickness calculated by both planar and 3D methods in these three regions were compared in slices from base to apex.

5.4 Statistical analysis

Student's paired t-tests were used to compare planar and 3D wall thickness measurements at each of the defined slice levels. Wall thickness normal bands were computed based on the 20 normal individuals with both the planar and 3D methods. Normal ranges were defined by the mean plus/minus twice the standard deviation (SD) to approximate the 95% probability interval.

5.5 Results

5.5.1 Phantom study

Figure 5-6 shows a comparison between the wall thickness results computed by the 3D and 2D methods for the slices 2, 3, 5 and 7 of the software phantoms. The planar (2D) measurements (left column) demonstrate an obvious overestimation of true wall thickness in those phantoms which have been positioned at an oblique angle with the imaging plane. In slice 7 one can see that wall thickness is rather accurately calculated in the true short-axis phantom (at zero degrees in each graph), but that both average and maximum measured wall thickness values rapidly increase when the phantoms become more angulated with respect to the short-axis orientation. The wall thickness results acquired with the 3D method do not display such overestimation, not even in the phantom with the largest angulation of 60° to the true short-axis orientation. The precision of the individual 2D centerline measurements is expressed in terms of the standard deviation calculated over the one hundred measurement chords in each phantom image. At all four slice levels, this standard deviation increases when examining phantoms at increasing

acquisition angles. In contrast, results assessed with the 3D method demonstrate a standard deviation which is insensitive to acquisition angle, and is therefore generally much lower than comparable planar measurements.

Table 5-1. Wall thickness (in mm) in five software phantoms at an approximately short-axis orientation

Angle	*Dimension*	*Slice 2 (Apical) Mean (±SD)*	*Slice 3 (Low) Mean (±SD)*	*Slice 5 (Mid) Mean (±SD)*	*Slice 7 (Basal) Mean (±SD)*
0 º	2D	12.8 (0.41)	11.2 (0.28)	10.5 (0.35)	10.0 (0.24)
	3D	11.0 (0.34)	10.1 (0.26)	10.3 (0.33)	10.0 (0.24)
5º	2D	12.9 (0.56)	11.2 (0.42)	10.4 (0.30)	9.9 (0.33)
	3D	11.1 (0.33)	10.1 (0.35)	10.3 (0.28)	9.9 (0.33)
10 º	2D	13.0 (0.66)	11.1 (0.59)	10.4 (0.30)	10.1 (0.30)
	3D	11.2 (0.34)	10.1 (0.30)	10.2 (0.26)	10.0 (0.31)
15 º	2D	12.7 (1.02)	11.2 (0.71)	10.4 (0.33)	10.2 (0.33)
	3D	11.0 (0.38)	10.1 (0.36)	10.2 (0.30)	10.1 (0.30)
20 º	2D	12.8 (1.11)	11.0 (0.73)	10.5 (0.40)	10.2 (0.31)
	3D	11.1 (0.39)	9.9 (0.36)	10.2 (0.24)	9.9 (0.26)

Planar and three-dimensional wall thickness figures in mm from five near short-axis software phantoms at different inclinations with the imaging plane, as mean (± SD). The angles denote the deviation from the short-axis orientation. Overall true phantom wall thickness was 10.0 mm.

The effect of the curvature of the myocardium towards the apex, the second possible cause of overestimation in 2D assessed wall thickness, may be isolated from the aforementioned effects by only examining the true short-axis phantom at different slice levels. Figure 5-6 demonstrates that 2D acquired average wall thickness in this phantom displays the largest overestimation of true wall thickness in slices close to the apex (shown for slice 2). Table 5-1 lists the wall thickness results in phantoms up to 20° from the short-axis orientation in tabular form. It shows that at a 10° deviation from the true short-axis orientation for example, which may be considered comparable to clinical practice, measured wall thickness varied from 10.1 mm to 12.5 mm (mean 11.1 mm) at slice 3, and from 11.8 to 14.3 mm (mean 13.0 mm) for the apical slice 2. In comparison to the phantom true wall thickness of 10.0 mm, maximum errors of up to 43% at the apex (mean error 30%) occur. The 3D measurements significantly reduced this error to mean values of 12% and 1% for slices 2 and 3, respectively.

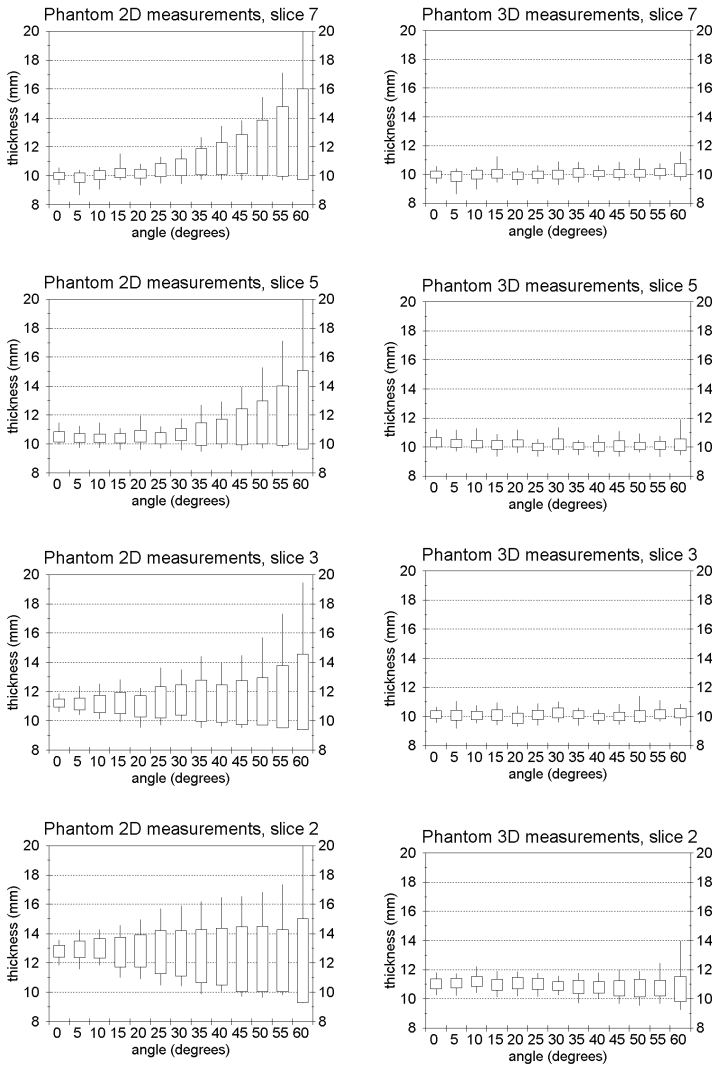

Figure 5-6. Two-dimensional (2D) and three-dimensional (3D) measurements from software phantoms at angulations between 0° and 60° from the short-axis orientation. The graphs on the left (A, C, E, G) display the results for the 2D measurements for slice 7, 5, 3, and 2 respectively; on the right (B, D, F, H) the corresponding results for the 3D measurements are shown.

5.5.2 In-vivo study

Table 5-2 lists the wall thickness measurements from 20 normal individuals by both the 2D and 3D methods, performed at each slice level (Apical / Low / Mid / Basal) in the two cardiac phases (ED/ES). The difference between both methods is also expressed as a percentage decrease in measured wall

thickness implied by the 3D method's correction. All these differences including those at the highest slice level were statistically significant ($p<0.05$). Table 5-2 also lists the standard deviation (SD) of the 100 measurement chords within each single image, averaged over the 20 individuals. The 3D method also results in a smaller standard deviation compared to the 2D measurements, as is shown by the percent difference between the methods.

Table 5-2. Wall thickness at four levels in 20 healthy volunteers

	Apical	Low	Mid	High
ED	Mean (SD)	Mean (SD)	Mean (SD)	Mean (SD)
2D [mm]	6.52 (1.00)	6.92 (0.93)	7.09 (0.87)	7.62 (0.92)
3D [mm]	5.79 (0.77)	6.32 (0.84)	6.90 (0.87)	7.56 (0.91)
Diff. [%]	11.24* (22.90)	8.67* (10.13)	2.57* (0.31)	0.73* (0.90)
ES				
2D [mm]	11.43 (2.18)	12.90 (1.96)	13.30 (2.07)	12.84 (1.81)
3D [mm]	10.63 (1.90)	12.22 (1.73)	12.97 (1.92)	12.73 (1.79)
Diff. [%]	6.96* (12.89)	5.28* (11.64)	2.51* (7.44)	0.92* (1.47)

Mean (in-slice SD) wall thickness in 20 healthy volunteers, and the percent difference in mean between the 2D and 3D methods. Both mean and SD were lower when calculated in 3D (* $p<0.05$).

The differences between both methods in average wall thickness are also reflected in the normal value graphs for the low and apical slice levels (Figure 5-7). In these graphs the normal values have both smaller ranges as well as a lower average value when assessed in 3D compared to the planar method. It is also shown however, that this observed global difference between the 3D and 2D thickness methods is not equally large in different regions along the myocardial circumference. As a result, the 3D graphs show a much more homogeneous wall thickness pattern along the myocardial circumference compared to the planar measurements.

When the myocardial circumference is divided into three distinct anatomical regions, it is apparent that regional planar wall thickness results are increasingly different in slice levels close to the apex, whereas the 3D results are not (Figure 5-8). In all slices, the septal region displays almost identical planar and 3D results, while the anterior region shows very different results computed by the planar and 3D methods.

Overall it can be observed that the large wall thickness inhomogeneity associated with the planar measurements is decreased by applying the WT3D method. There is, however, a difference between ED and ES in percentage wall thickness decrease imposed by the 3D method, which makes this decrease in inhomogeneity much less obvious at ES.

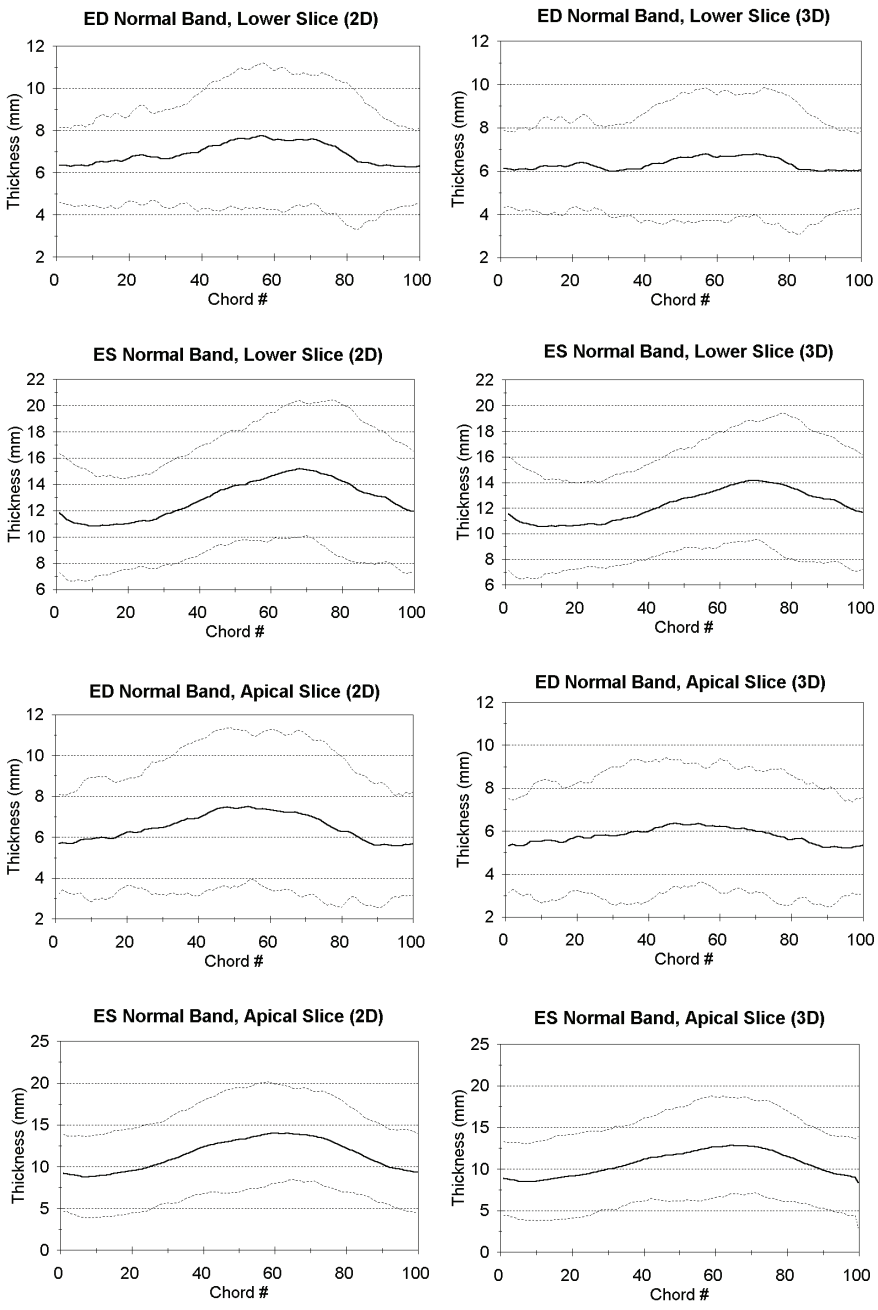

Figure 5-7. The normal wall thickness values in the end-diastolic (ED) and end-systolic (ES) phases determined from the 20 healthy volunteers plotted for two-dimensional (A, C, E, G) and three-dimensional (B, D, F, H) measurements in the lower slice and the apical slice.

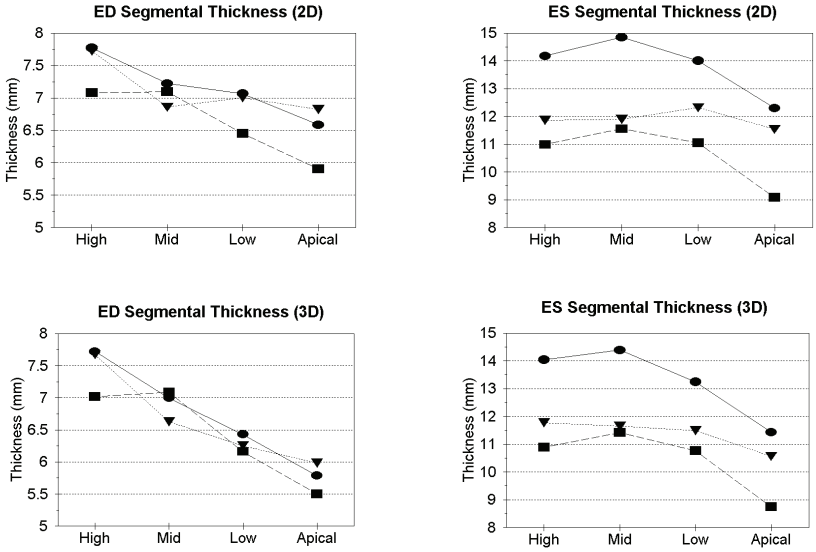

Figure 5-8. Wall thickness values for the individual anatomical regions (septal= chord 1-20; anterior = 21-50; lateral/posterior = 51-100). Results are shown for two-dimensional (top row) and three-dimensional (bottom row) measurements in the end-diastolic and end-systolic phases.

5.6 Discussion

The three-dimensional nature of a multi-slice, multi-phase short-axis MR acquisition of the left ventricle makes it an excellent choice for assessing regional functional parameters, such as wall thickness and thickening or thinning. Straightforward 2D wall thickness measurements within the imaging plane however, overestimate true thickness depending on the location of the measurement along the myocardial wall.

5.6.1 Accuracy of 3D wall thickness assessment

In order to accurately estimate true myocardial wall thickness, a 3D wall thickness calculation algorithm was developed and evaluated. Since the algorithm was based on a correction of the planar measurements by the known improved centerline method, a high planar resolution was achieved. In addition, 2D and 3D measurements could be performed at identical positions along the myocardium enabling a one-to-one comparison of 2D and 3D measurements. Planar wall thickness measurements with the Improved Centerline method on the ventricular shaped phantoms confirmed the expected inaccuracies of the planar method. At the apical slice wall thickness was systematically overestimated, and in the phantoms

with a tilt relative to the imaging plane an increase in random error was observed. In contrast, the developed 3D method did accurately estimate true wall thickness, independent of slice location and long-axis orientation. At places where the imaging plane was indeed perpendicular to the phantom's myocardium, and the 2D centerline method was thus a good measure of the true wall thickness, the correction by the 3D method was minimal and results similar to the 2D measurements were obtained. At the level of the most apical slice, the 3D method was only able to compensate for approximately half the planar error. This is caused by the myocardial surface model used in the calculations, which only extends as far as the acquired basal and apical slices. Local, vertical myocardial curvature at these outer slices could therefore not accurately be estimated. Extrapolation of the surface model towards the apex based only on the visible epicardium might solve this problem. However, special care should be taken not to introduce new errors into the results.

5.6.2 Alternative solutions to 3D wall thickness assessment

The need to use 3D techniques to accurately estimate true wall thickness from multi-slice short-axis acquisitions has been reported earlier[16-18]. Specific implementations of such techniques have been suggested, all of which based on volume element algorithms. These volume element algorithms partition the myocardium into relatively large myocardial volumetric segments, often in-between the image slices, and derive average wall thickness for each element from its volume and geometric assumptions about its shape. Volumetric methods further define myocardial segments in each myocardial volume ring by either an MR radial tagging acquisition protocol[18,19] or software generated radii from a given ventricular center point[16]. The number of segments thus defined along the circumference of the myocardium is limited, for example to 8, 12 or 16 segments[17,18,20]. Applied to image material from this study only the latter method would achieve an in-slice measurement sampling rate that is comparable to the 10 mm distance between the imaging slices.

A minimum requirement for any wall thickness assessment method must be a correct mapping of myocardial segments to a distribution map of the coronary arteries in order to enable a correlation between impaired myocardial function and reduced coronary arterial supply. In practice, this mapping is very difficult to obtain in a straightforward fashion, and is therefore substituted by a mapping based on anatomical features obtained from the image[21]. To facilitate an accurate mapping of myocardial segments, and to prevent obscuring of small details in the regional functional analysis due to the averaging process, a sufficiently high planar

sampling resolution is required. The presented 3D method makes use of the high image resolution present by performing 100 measurements per image, and thereby facilitates a more than accurate mapping to anatomical features in the image.

5.6.3 Effects of 3D assessment on the normal population results

The greater 3D circumferential wall thickness homogeneity within imaging slices of the normal population was in accordance with the expectations dictated by theory and the phantom experiments. This phenomenon is also in accordance with reports from Beyar[16,17], whose experiments on normal canine hearts also demonstrated a lower standard deviation per slice when thickness was measured in three dimensions.

Figure 5-8 demonstrated that the difference between planar and 3D methods is largest at the anterior region, most likely due to a larger myocardium-to-imaging plane inclination compared to other myocardial regions. In contrast, almost no difference between both wall thickness methods exists in the septal region, where myocardial wall and imaging plane can be expected to be almost perpendicular. It is thus shown that planar wall thickness measurements are likely to randomly overestimate regional thickness even in optimally acquired, true short axis acquisitions.

Although the 3D method decreased differences in normal wall thickness between different myocardial segments, it could not be attributed to significantly smaller normal bands. Differences in myocardial wall inclination therefore can not be a main cause for planar thickness variation between normal subjects. The wide range in normal thickness results is thus more likely attributed to differences in each normal individual's anatomy associated with age and physical condition which were not explicitly defined in this study.

5.6.4 3D assessed wall thickening

Wall thickening is a well known measure for local myocardial function, and is superior to other methods such as wall motion in discriminating between normal and dysfunctional myocardium when calculated in-plane[9] as well as in three dimensions[20]. It is, however, very sensitive to the accuracy of wall thickness measurements, especially in the end-diastolic phase[11]. Application of more accurate 3D wall thickness assessment may thus be advantageous in achieving a more accurate description of cardiac function.

5.7 Conclusion

A new 3D wall thickness method has been developed which demonstrated the ability to estimate true wall thickness in phantom studies with a higher accuracy and precision than current planar methods. The method makes use of the well-established, accurate 2D improved centerline method and therefore performs measurements at a high planar resolution. It exploits the 3D information present in multi-slice, multi-phase short-axis MR images of the left ventricle, providing a detailed insight into local left ventricular functioning. Application of the 3D method to short-axis MR studies of 20 healthy volunteers has shown an increase in wall thickness homogeneity along the circumference of the LV wall, leading to more homogeneous wall thickness normal values at each individual slice level. The use of a 3D method is an essential prerequisite for the derivation of accurate wall thickness normal data from a population of normal individuals, and may also be important in the assessment of regional wall thickening.

5.8 References

1. Dinsmore RE, Wismer GL, Miller SW, Thomson R, Johnston DL, Liu P, Okada RD, Saini S, Brady TJ. Magnetic resonance Imaging of the heart using imaging planes oriented to cardiac axes: experience with 100 cases. AJR 1985; 145:1177-1183.
2. Buser PT, Auffermann WW, Holt WW, Wagner S, Kircher B, Wolfe C, Higgins CB. Noninvasive evaluation of global left ventricular function with use of cine nuclear magnetic resonance. J Am Coll Cardiol 1989; 11:1294-1300.
3. Semelka RC, Tomei E, Wagner S, Mayo J, Kondo C, Suzuki J, Caputo GR, Higgins CB. Normal left ventricular dimensions and function: Interstudy reproducibility of measurements with cine MR imaging. Radiology 1990; 174:763-768.
4. Shapiro EP, Rogers WJ, Beyar R, Soulen RL, Zerhouni EA, Lima JAC, Weiss JL. Determination of left ventricular mass by magnetic resonance imaging in hearts deformed by acute infarction. Circulation 1989; 79:706-711.
5. Pattynama PMT, Lamb HJ, van der Velde EA, van der Wall EE, de Roos A. Left ventricular measurements with cine and spin-echo MR imaging: a study of reproducibility with variance component analysis. Radiology 1993; 187:261-268.
6. Fisher MR, von Schulthess GK, Higgins CB. Multiphasic cardiac magnetic resonance imaging: normal regional left ventricular wall thickening. AJR 1985; 145:27-30.
7. Haag UJ, Maier SE, Jakob M, Liu K, Meier D, Jenni R, Boesiger P, Anliker M, Krayenbuehl HP. Left ventricular wall thickness measurements by magnetic resonance: a validation study. Int J Cardiac Imag 1991; 7:31-41.
8. van Rugge FP, van der Wall EE, Spanjersberg SJ, de Roos A, Matheijssen NAA, Zwinderman AH, van Dijkman PRM, Reiber JHC, Bruschke AVG. Magnetic resonance imaging during dobutamine stress for detection of coronary artery disease; quantitative wall motion analysis using a modification of the centerline method. Circulation 1994; 90:127-138.

9. Holman ER, Vliegen HW, van der Geest RJ, Reiber JHC, van Dijkman PRM, van der Laarse A, de Roos A, van der Wall EE. Quantitative analysis of regional left ventricular function after myocardial infarction in the pig assessed with cine magnetic resonance imaging. Magn Reson Med 1995; 34:161-169.
10. Baer FM, Smolarz K, Theissen P, Voth E, Schicha H, Sechtem U. Regional 99mTc-methoxyisobutyl-isonitrile-uptake at rest in patients with myocardial infarcts: comparison with morphological and functional parameters obtained from gradient-echo magnetic resonance imaging. Eur Heart J 1994; 15:97-107.
11. Lamb HJ, Singleton RR, van der Geest RJ, Pohost GM, de Roos A. MR imaging of regional cardiac function: Low-pass filtering of wall thickness curves. Magnetic Resonance in Medicine 1995; 34:498-502.
12. van der Geest RJ, Jansen E, Buller VGM, Reiber JHC. Automated detection of left ventricular epi- and endocardial contours in short-axis MR images. Comput Cardiol 1994:33-36.
13. von Land CD, Rao SR, Reiber JHC. Development of an improved centerline wall motion model. Comput Cardiol 1990: 687-690.
14. Sheehan FH, Bolson EL, Dodge HT, Mathey DG, Schofer J, Woo HK. Advantages and applications of the centerline method for characterizing regional ventricular function. Circulation 1986; 74:293-305.
15. Goodyer AVN, Langou RA. The multicentric character of normal left ventricular wall motion: implications for the evaluation of regional wall motion abnormalities by contrast angiography. Cathet Cardiovasc Diagn 1982; 8:325-232.
16. Beyar R, Shapiro EO, Graves WL, Rogers WJ, Guier WH, Carey GA, Soulen RL, Zerhouni EA, Weisfeldt ML, Weiss JL. Quantification and validation of left ventricular wall thickening by a three-dimensional volume element magnetic resonance imaging approach. Circulation 1990; 81:297-307.
17. Beyar R, Weiss JL, Shapiro EP, Graves WL, Rogers WJ, Weisfeldt ML. Small apex-to-base heterogeneity in radius-to-thickness ratio by three-dimensional magnetic resonance imaging. Am J Physiol 1993; 264 (Heart Circ. Physiol. 33):H133-H140.
18. Lima JA, Jeremy R, Guier W, Guier W, Bouton S, Zerhouni EA, McVeigh E, Buchalter MB, Weisfeldt ML, Shapiro EP, Weiss JL. Accurate systolic wall thickening by NMR imaging with tissue tagging: correlation with sonomicrometers in normal and ischemic myocardium. J Am Coll Cardiol 1993; 21:1741-1751.
19. Dong SJ, MacGregor JH, Crawley AP, McVeigh E, Belenkie I, Smith ER, Tyberg JV, Beyar R. Left ventricular wall thickness and regional systolic function in patient with hypertrophic cardiomyopathy A three-dimensional tagged magnetic resonance imaging study. Circulation 1994; 90:1200-1209.
20. Azhari H, Sideman S, Weiss JL, Shapiro EP, Weisfeldt ML, Graves WL, Rogers W, Beyar R. Three-dimensional mapping of acute ischemic regions using MRI: wall thickening versus motion analysis. Am J Physiol 1990; 259 (Heart Circ. Physiol. 28):H1492-H1503.
21. Schiller NB, Shah PM, Crawford M, et al. Recommendations for quantification of the left ventricle by two-dimensional echocardiography. J Am Soc Echocard 1989; 2:358-367.